Nuclear Engineering and Design 241 (2011) 2075–2085

Contents lists available at ScienceDirect

Nuclear Engineering and Design

journal homepage: www.elsevier.com/locate/nucengdes

Very-Large Eddy Simulation (V-LES) of the flow across a tube bundle

Mathieu Labois, Djamel Lakehal*

ASCOMP GmbH, Technoparkstrasse 1, CH-8005 Zürich, Switzerland

ARTICLE INFO

Article history:
Received 14 September 2010
Received in revised form 15 February 2011
Accepted 18 February 2011

ABSTRACT

A new turbulence modelling approach (Very-Large Eddy Simulation; V-LES) is developed and compared to conventional RANS and LES for a flow across a tube bundle. The method, which belongs to the large-scale simulation category, represents a good compromise between efficiency and precision, and may thus be used for industrial problems for which LES remains computationally expensive under high to very-high Reynolds number flow conditions. It can also be used for gas–liquid two-phase flows such as pressurized thermal shocks. The method is a sort of blend between U-RANS and LES, in that it resolves very large structures – way larger than the grid size – and models all subscale of turbulence using a two-equation model, by reference to RANS. The original model is shown here to share the same characteristics as the Detached Eddy Simulation (DES) approach, in that when the filter width is smaller than the wall-distance at which viscous effects are negligible ($f_\mu = 1$), the fixed filter width is replaced by the wall distance. First conclusions to be drawn from its extension here is that the flow must be resolved in three-dimensions, under transient conditions, with refined grids. Sensitivity to various computational parameters has been addressed: grid, filter width, domain size, and inflow conditions. This modelling strategy is proved to provide the flow unsteadiness in three-dimensions, while saving computational cost compared to LES. The method is computationally efficient (it can be applied using an implicit solver which permits a higher CFL than with LES; typically 1 versus 0.1), and numerically robust. The computational cost decreases with increasing filter width, though at the expenses of the quality of the results.

© 2011 Elsevier B.V. All rights reserved.

1. Introduction

For many thermal-hydraulics problems and pressurized thermal shocks (PTS) in particular, it is important for the simulation to represent correctly the turbulent-induced motions of fluids processes. The very popular k–ε model has been shown to be unable to predict this type of flows accurately (Johansen et al., 2004; Johnson, 2008), although the predicted zero- and first-order mean quantities (e.g. velocities) are acceptable. Various studies have shown that Reynolds stresses are under-estimated by the standard model.

A substantial amount of work has recently been undertaken to simulate the flow across tube bundles using Large Eddy Simulation or even more precise methods such as Direct Numerical Simulation (Moulinec et al., 2004). Results are in general much better than with RANS and are globally in good agreement with experimental data (Rollet-Miet et al., 1999; Benhamadouche and Laurence, 2003; Hassan and Barsamian, 2004; Moulinec et al., 2004). However, very fine grids are needed to perform statistically resolved LES together with a substantial amount of data to conduct statistical analysis and infer times averaged data. Be it as it may, LES is very costly in terms of computational power, in particular when applied for high Reynolds number practical flow problems.

Over the last years new approaches have been proposed to precisely reduce the cost of LES while keeping the fundamental unsteady aspect of the method intact, in order to find a compromise between efficiency and accuracy of the numerical methods. Other variants have been recently invoked, including the SAS model implemented in CFX. The Very-Large Eddy Simulations approach (V-LES) has originally been proposed by Speziale (1998). It has been lately reformulated by Ruprecht et al. (2003) and Johansen et al. (2004) such as it becomes based on the concept of filtering the turbulent scales produced by RANS. The outcome is a sort of unsteady, three-dimensional turbulence model, acting as a link between the Unsteady Reynolds Averaged Navier–Stokes (U-RANS) using the standard k–ε model and LES. This concept is very promising since it offers a good compromise between efficiency and precision, and may thus be used for industrial problems for which LES remains computationally out of reach of many users. The method – under its original as well as filter-based variants – which is gaining in popularity has been successfully applied to predict a wide range of high Re flows, e.g. the flow across a square cylinder by Johansen et al. (2004).

In this paper, the V-LES is systematically assessed for the flow across a tube bundle, and results are compared – together with

* Corresponding author.
E-mail address: lakehal@ascomp.ch (D. Lakehal).

0029-5493/$ – see front matter © 2011 Elsevier B.V. All rights reserved.
doi:10.1016/j.nucengdes.2011.02.009

full LES – against the measurement data of Simonin and Barcouda (1986). In the next section, the different turbulence models that have been used in this study are presented. Then, we will present the test case of a flow around a tube bundle, together with numerical details. In the following section, the influences on the results of different computational parameters are evaluated, so that useful guidelines can be proposed for treating this class of flow.

2. Turbulent flow modelling

The objective of this piece of work is to simulate an incompressible turbulent flow across a staggered tube bundle, based on the experiment of Simonin and Barcouda (1986). The incompressible Navier–Stokes equations are employed, with three different modelling strategies: the standard k–ε RANS model, V-LES and LES models. The standard k-epsilon model (Launder and Spalding, 1974) is first used for the modelling of turbulence under steady-state conditions. The well-known mode consists in solving two additional equations for the turbulent kinetic energy k and its rate of dissipation ε. The model equations are well-known and do not require to be presented here.

2.1. Very Large Eddy Simulation

Very-Large Eddy Simulation (V-LES) is based on the concept of filtering a larger part of turbulent fluctuations as compared to LES (as the name clearly implies). This directly necessitates the use of a more complex sub-grid modelling strategy. The V-LES used in this study is based on the use of k–ε model as a sub-filter model. The filter width is no longer related to the grid size; instead it can be chosen to be any length scale larger than the grid size, but necessarily smaller than the characteristics macro length scale of the flow (e.g. tube diameter). Increasing the filter width beyond the largest length scales will lead to predictions similar to the standard RANS model, whereas in the limit of a small filter-width (approaching the grid size) the model predictions should tend towards those of LES. V-LES could thus be understood as a natural link between conventional LES and U-RANS, i.e. a useful compromise between model accuracy and computational cost for industrial single and multiphase flow. As mentioned above the V-LES as used and implemented in TransAT is based on the k–ε model to treat sub-scale turbulence, or to model the diffusive effect of flow motions smaller in size than the specified filter width. If the filter width is smaller than the length scale of turbulence provided by the RANS model, then larger turbulent flow structures will be able to develop during the simulation, depending on the grid resolution and simulation parameters (in particular regarding time stepping and the order and accuracy of the time marching schemes employed).

The V-LES theory as currently used has been proposed by Johansen et al. (2004). We will briefly present this theory; for a more detailed presentation and a discussion on the values of the model constants, the reader can refer to the original paper. The filter width will be noted as Δ in the following. The Kolmogorov equilibrium spectrum is supposed to apply to the sub-filter flow portion. Thus, the isotropic RMS velocity for the sub-filter flow can be written as follows:

$$u'_\Delta = \sqrt{\frac{3}{2}}\kappa_\Delta^{3/2} = \int_{k_\Delta}^{\inf} \Phi(\kappa)d\kappa = C_k^{1/2}\kappa_\Delta^{-1/3}\varepsilon^{1/2}. \quad (1)$$

where κ stands for the wave number. The RMS velocity wave number spectrum $\phi(\kappa)$ is identified to $C_k^{1/2}\kappa_\Delta^{-1/3}\varepsilon^{1/2}$, with the constant $C_k = 1.62$ following Smith and Woodruff (1998). The cut-off wave length is related to the double filter size by $\kappa_\delta = 2\pi/2\delta$. The isotropic turbulent viscosity can then be defined using

$$\left(u'_\Delta \cdot l\right) = \int_{k_\Delta}^{\inf} \Phi(\kappa)\frac{\pi}{\kappa}d\kappa = \frac{\pi}{3}C_k^{1/2}\varepsilon^{1/3}\int_{k_\Delta}^{\inf}\kappa^{-7/3}d\kappa = u'_\Delta\frac{\Delta}{4}. \quad (2)$$

Defining the anisotropic factor $\gamma < 1$, the turbulent viscosity is rewritten as $\nu_t = \gamma u'_\Delta \Delta/4$ so that anisotropic effects can be taken into account. In the limit of a very large filter width, the effective length scale is limited upwards by

$$l_{\text{eff}} \equiv \nu_t/u'_\Delta = C_\mu\sqrt{\frac{3}{2}}k^{3/2}/\varepsilon. \quad (3)$$

which enables to re-write the viscosity of the filtered model under the form

$$\nu_t = \nu_{t,\text{RANS}} f(C_3\Delta\varepsilon k^{-3/2}). \quad (4)$$

where $C_\mu = 0.09$ is the usual model constant and C_3 is a new model constant introduced by Johansen et al. (2004). The length-scale limiting function f has the following properties

$$f(C_3\Delta\varepsilon k^{-3/2}) = \begin{cases} 1 & \text{if } C_3\Delta\varepsilon/k^{3/2} \gg 1 \\ C_3\Delta\varepsilon/k^{3/2} & \text{otherwise} \end{cases}$$

This function cannot be known further if the entire energy spectrum is not explicitly known. Thus, the simple proposal from Johansen et al. (2004) is used here

$$f(C_3\Delta\varepsilon k^{-3/2}) = \min\left|1, C_3\Delta\varepsilon/k^{3/2}\right|. \quad (5)$$

Near the wall boundaries, the function is forced to be equal to 1, which means that the standard k–ε model is systematically applied in these regions, an artefact that permits the use of the standard wall-functions in the V-LES context, too. The method can also be employed under low-Re flow conditions, using either a two-layer approach based on a one-equation model or full integration down to the viscous sublayer; i.e. Low-Re model. Finally, the turbulent viscosity for V-LES can be written as,

$$\nu_t = C_\mu\frac{k^2}{\varepsilon}C_3\frac{\Delta\varepsilon}{k^{3/2}}. \quad (6)$$

The difference between RANS, LES and V-LES, is that in the latter approach, it is necessary to specify a filter width, which can be made proportional to a length-scale characteristics of the flow under consideration, e.g. cylinder diameter. This parameter will be the object of a numerical study in Section 4 in order to evaluate its influence and give some information about the way it should be specified. Apart from that, a lower bound must be set to ensure that the filtering process is compatible with the grid resolution. Practically we impose $\Delta > 1.5\,\Delta_{\text{grid}}$ where $\Delta_{\text{grid}} = (\Delta_x\Delta_y\Delta_z)^{1/3}$ for a three-dimensional grid.

It is perhaps important to note that the subscale model above (6) is in itself a blend between a one-equation model and a two-equation variant. Near the wall, when the specified length scale Δ is smaller than wall distance, the subscale model degenerates to the DES approach (detached Eddy Simulation), whereby the wall layer is resolved using a one-equation model (in which case other approaches like the Spalart and Allmaras (1992) model could be used). In the outer flow, in the limit of $(\Delta\varepsilon/k^{2/3} \gg 1)$, the subscale model tends however to recover the k–ε approach, somehow attenuated by coefficient C_3.

The original model of Johansen et al. (2004) forces the subscale model to treat near-wall regions using the standard k–ε model, such as wall functions could be employed. We could actually show that at the limit of wall distances (y_n) at which viscous effects become negligible, i.e. when $f_\mu = 1$, Eq. (6), which takes the form

$\nu_t = C_\mu C_3 \Delta k^{1/2}$ for $(\Delta\varepsilon/k^{2/3} \ll 1)$ should rather be re-cast in the form of a Prandtl mixing length model: $\nu_t = C_\mu L_\mu k^{1/2}$, where the length scale (L_μ) could be defined for example by reference to Norris and Reynolds, 1975 – or another model: $L_\mu = C_1 y_n f_\mu$, with the damping function $f_\mu = 1 - \exp(-R_y/A_\mu)$ and C_1 is a model coefficient to be set to conform with the logarithmic law of the wall. If in this viscosity-affected layer the transport equation of the rate of dissipation is disregarded in favour of an algebraic prescription (e.g. $\varepsilon = k^{3/2}/L_\varepsilon$,), the final model degenerates to a two-layer model (Lakehal and Thiele, 2001), which in the context of coupled LES-RANS is commonly known as DES, short for Detached Eddy Simulation.

2.2. Large Eddy Simulation

Large Eddy Simulation is based on the concept of directly solving for all turbulent length scales that can be resolved (larger than the grid size) in a given mesh and modelling the effect of the sub-grid scales on the resolved-scale evolution. However, arbitrarily coarse grids cannot be used for LES due to the assumptions put forward while developing the sub-grid scale models; namely: small-scale isotropy, independence of the SGS scales from the boundary and inflow conditions and diffusive, dissipative characteristics. The number of grid points needed for an accurate LES scales non-linearly with the Reynolds number. This makes LES currently too expensive for industrial turbulent flows. The LES or filtered Navier–Stokes equations are now well-known; we thus restrict the presentation of the approach to the SGS model employed.The WALE model of Nicoud and Ducros (1999) has been used for SGS modelling in the present context; it defines the SGS eddy viscosity as

$$\nu_t = (C_w \Delta)^2 \frac{(S^d_{ij} S^d_{ij})^{3/2}}{(\bar{S}_{ij}\bar{S}_{ij})^{5/2} + (S^d_{ij} S^d_{ij})^{5/4}}. \quad (7)$$

where $C_w = \sqrt{10.6 {C_s}^2}$, and ${S^d}_{ij}$ reads:

$$S^d_{ij} = \frac{1}{2}(\bar{g}^2_{ij} + \bar{g}^2_{ji}) - \frac{1}{3}\delta_{ij}\bar{g}^{-2}_{kk};\ \bar{g}_{ij} = \frac{\partial \bar{u}_i}{\partial x_j};\ \text{and}\ \bar{g}^2_{ij} = \bar{g}_{ik}\bar{g}_{kj}$$

where δ_{ij} is the Kronecker symbol. In the current simulations, the Smagorinsky constant C_S is assigned the value of 0.08, and the filter width Δ is set equal to $2\Delta_{\text{grid}}$. The model has been shown to behave very well in wall-bounded flows, without a specific damping function a la van Driest. It has also been shown to be less dissipative and capture the thin-shear layer pretty accurately.

3. Flow across a cyclic tube bundle

3.1. Presentation of the test case

Our numerical simulations will be compared with the experiment of Simonin and Barcouda (1986), who studied the flow across a staggered tube bundle with diameter $D = 21.7$ mm. The flow Reynolds number, based on the diameter of the tube, is 18,000, and the bulk velocity is 1 m/s. This flow has a complex behaviour, non-homogeneous and inherently unsteady, with a flapping effect in the wake of the bundles. Simonin and Barcouda (1986) provide mean velocities in the x and y directions, as well as the Reynolds stresses $\langle u'u' \rangle$, $\langle v'v' \rangle$, and shear stress $\langle u'v' \rangle$ for different locations. It should

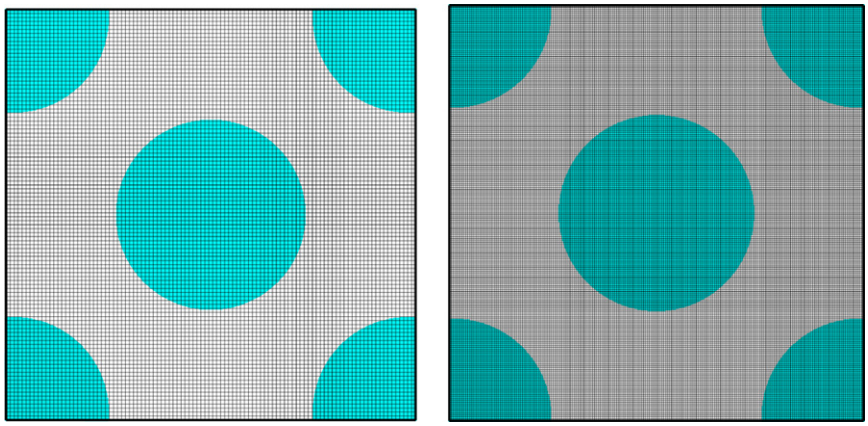

Fig. 1. 2D view of the computational domain using IST, with a mesh of 100 × 100 cells (left) and 200 × 200 cells (right).

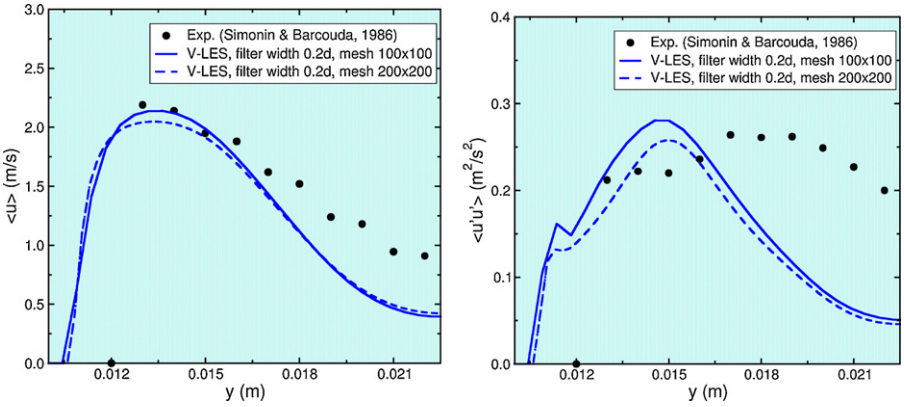

Fig. 2. Mean u-velocity and mean fluctuations at $x = 0$ mm for different mesh sizes. 2D simulations.

be noted that in several previous numerical simulations of this flow (e.g. Rollet-Miet et al., 1999; Benhamadouche and Laurence, 2003), smaller Reynolds number (9000 or less) were used to perform the simulations, otherwise the grid would have been considerably fine. On the other hand, Hassan and Barsamian (2004) used a slightly higher Reynolds number (21,700), and simulated the whole geometry, without using cyclic boundary conditions.

3.2. Numerical method

The C(M)FD code TransAT©developed at ASCOMP has been used for these simulations. The solver is a multi-physics type, based on fully conservative finite volumes for solving multi-fluid Navier–Stokes equations. It uses structured meshes, though allowing for multiple blocks to be set together. MPI parallel based algorithm is used in connection with multi-blocking. The grid arrangement is collocated and can thus handle more easily curvilinear skewed grids. The solver is pressure based (Projection Type), corrected using the Karki–Patankar technique for compressible flows (up to transonic flows). High-order time marching and convection schemes can be employed; up to third order monotone schemes in space. The second-order HLPA convection scheme has been employed for all the computations. For RANS and V-LES simulations, an implicit second-order Euler time stepping scheme is used, whereas an explicit second-order Euler scheme is used for LES.

3.3. Handling turbulence

TransAT has been employed with different turbulence models (RANS) and approaches (V-LES and LES). The LES results are considered to be the reference data, as the approach has been shown previously (e.g. Benhamadouche and Laurence, 2003) to provide simulation results in good agreement with the data. In LES, use is made of the SGS WALE (Nicoud and Ducros, 1999) model, with the Werner–Wengle wall-functions (TransAT User Manual, 2009). The LES simulations have been performed using an explicit time integration scheme of second-order. The RANS simulations have

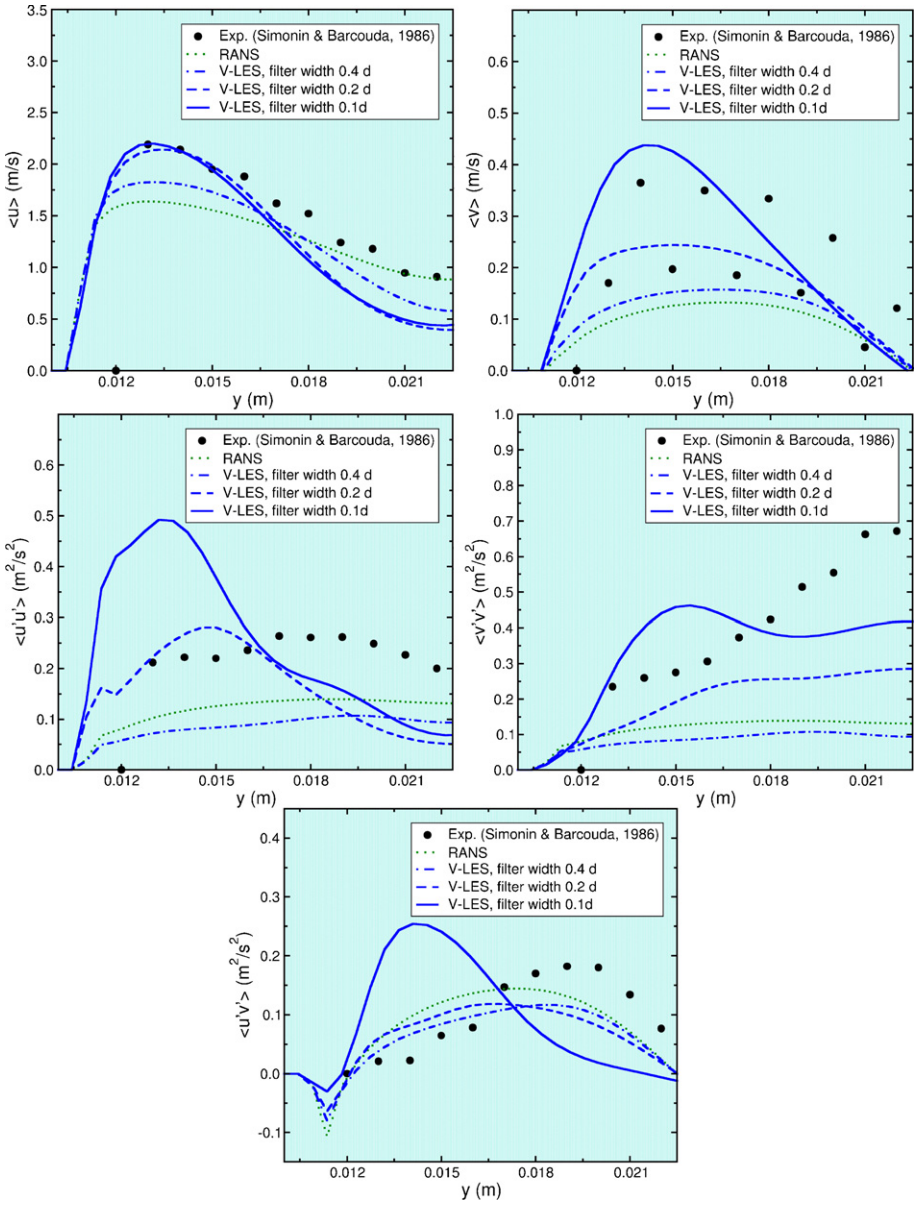

Fig. 3. RANS and V-LES results at $x = 0$ mm. 2D simulations.

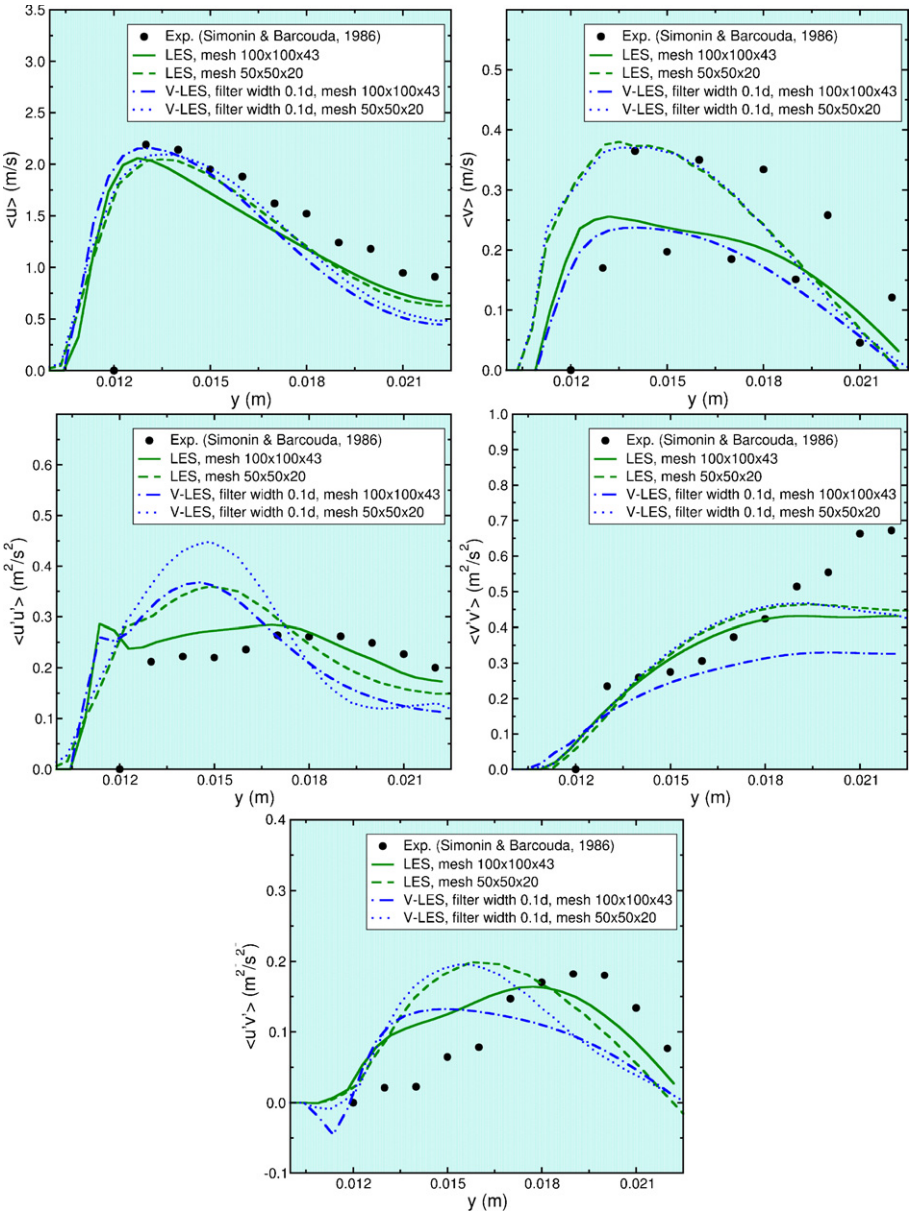

Fig. 4. Influence of the mesh size on the results: 3D simulations, results at $x = 0$ mm.

also been performed using the k–ε model, together with standard near-wall functions.

Finally, use is made of the V-LES approach to simulate turbulence in a precise and cost-efficient way as compared to RANS and LES. Because the V-LES encompasses a 2-equation model to treat subscale turbulence, an implicit time integration scheme has been used to perform the simulations, in contrast to LES, which required a 3rd order Runge–Kutta explicit time integration scheme. The approach should be implemented such that the base turbulence model employed for the subscales (be it a k–ε model or another type) is such that, applying a filter will prevent structures smaller than the specified filter size from being directly solved. The filter width in this model must be defined depending on the flow nature, on not on the grid size as in LES. Initial results using the k–ε model show that the integral turbulence length scale inferred using solved turbulent kinetic energy and dissipation values is about $0.8d$, with d being the tube diameter. To proceed, we have tested different filter widths falling in the interval 0.05–$0.4d$ to evaluate the influence of this parameter on the results.

3.4. Computational parameters

The computational domain is shown on Fig. 1; it has a dimension of 45 mm × 45 mm. The depth in the z-direction is one diameter when it is not mentioned. The origin is taken at the middle of the domain. Periodic boundary conditions are applied in the x and y directions, and in the z-direction when performing three-dimensional computations. As shown in figure, the grid is not of BFC type but of IST class; short for Immersed Surfaces Technology. In the IST the solid is described as the second 'component' or 'material', with its own thermo-mechanical properties. The technique differs substantially from the Immersed Boundaries method of Peskin (1972), in that the jump condition at the solid surface is implicitly accounted for, not via direct momentum forcing (using the penalty approach). It has the major advantage to solve conjugate heat transfer problems, in that conduction inside the body is directly linked to external fluid convection. The solid is first immersed into a cubical grid covered by a Cartesian mesh. The solid is defined by its external boundaries using the solid level set

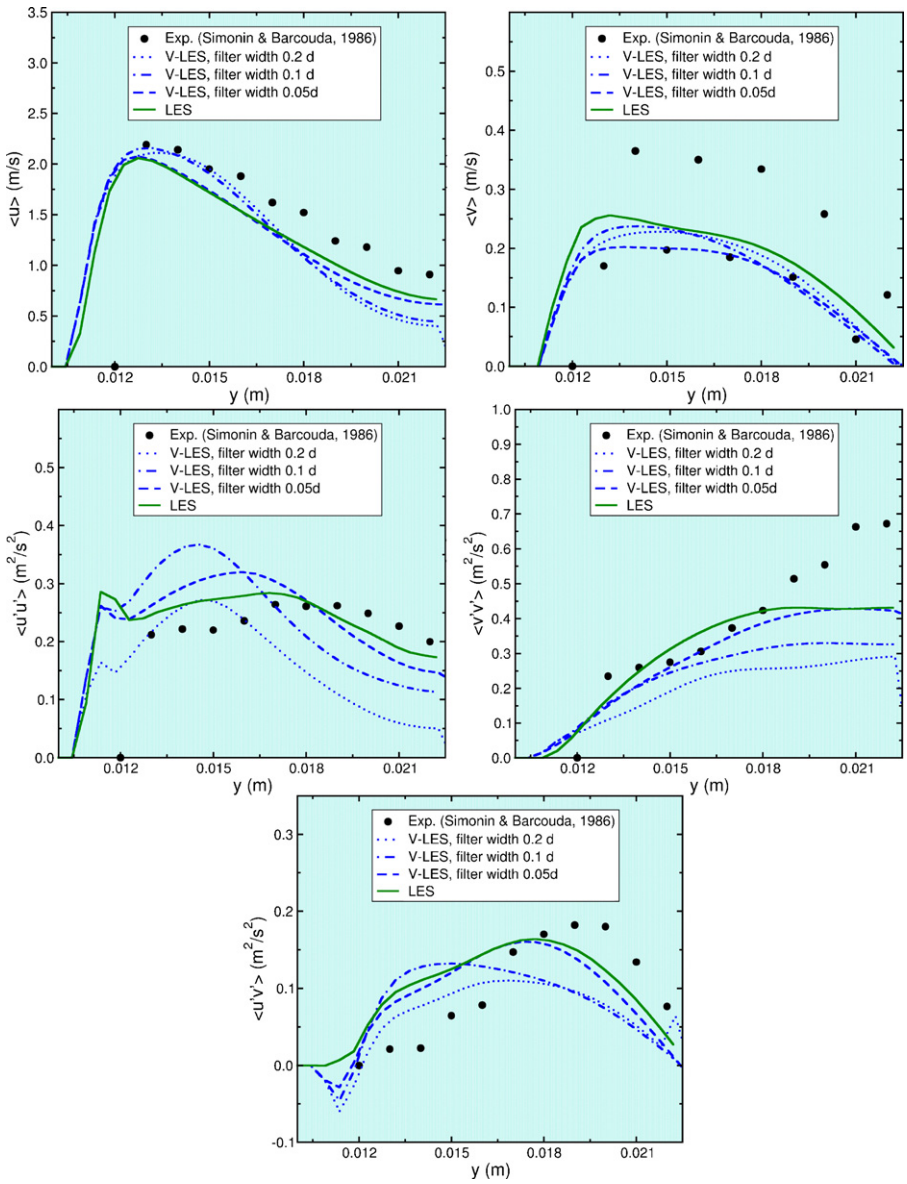

Fig. 5. Influence of the filter width on the results: 3D simulations, results at $x = 0$ mm.

function. Like in fluid–fluid flows, this function represents a distance to the wall surface; is zero at the surface, negative in the fluid and positive in the solid. The treatment of viscous shear at the solid surfaces is handled very much the same way as in all CFD codes.

A mean pressure forcing is applied in the x-direction to ensure that the bulk x-velocity (defined as the average of the velocity in the whole fluid domain) is 1.06 m/s. To match the experiments, the average of the velocities in the y and z-directions is set to zero. Fluid properties are set so that the Reynolds number based on this bulk velocity and tube diameter in effect equals 18,000.

Different mesh resolutions have been used in order to check grid dependency, with a number of cells in the x and y directions between 50 and 200. When three-dimensional computations are performed, the size of a cell in the z-direction is equal to the size in the other directions. These meshes have about the same precision as those used by Benhamadouche and Laurence (2003), who used unstructured grids of 2072 cells with refinements near the walls. The grid is coarser though than the two-dimensional meshes used by Johnson (2008), who used a grid of 14,976 cells.

3.5. Estimation of turbulent stresses

Experimental data of Simonin and Barcouda (1986) provide results at different locations for the mean velocities, as well as for the normal turbulent stresses $\langle u'u' \rangle$ and $\langle v'v' \rangle$, and the shear stress $\langle u'v' \rangle$. These normal and shear stresses must be evaluated during the different simulations, according to the turbulence model/approach considered. The expressions used to obtain these different results according to the model used are shown on Table 1.

Table 1
Expression of the numerical stresses used in the different models.

Experimental data	k–ε	V-LES	LES
$\langle u'u' \rangle$	$k/3$	$\overline{u'u'} + k/3$	$\overline{u'u'}$
$\langle v'v' \rangle$	$k/3$	$\overline{v'v'} + k/3$	$\overline{v'v'}$
$\langle u'v' \rangle$	$-2\mu_t \bar{S}_{ij}$	$\overline{u'v'} - 2\mu_t \bar{S}_{ij}$	$\overline{u'v'} - 2\mu_{SGS} \bar{S}_{ij}$

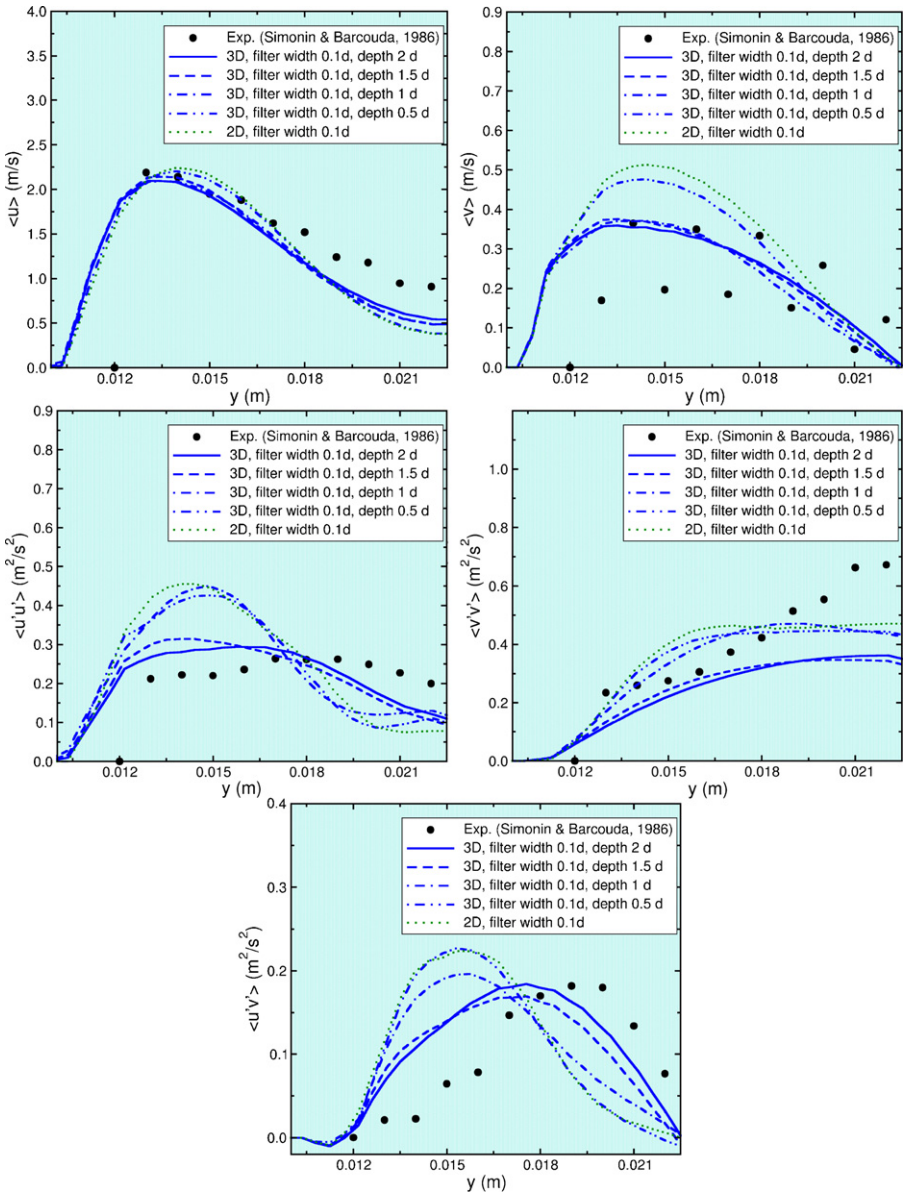

Fig. 6. Influence of the size of the computational domain in the spanwise direction: 3D simulations, results at $x = 0$ mm.

4. Results and discussion

4.1. 2D simulations

Two-dimensional simulations using V-LES have first been performed on meshes consisting of 100×100 and 200×200, respectively (see Fig. 1). The flow was established at $t = 0.3$ s when unsteady turbulent structures start to appear. Results are time-averaged between $t = 0.4$ s and $t = 0.8$ s. Results of the two grids for a filter width of $0.2d$ are shown in Fig. 2. The comparison shows actually that the 100×100 grid may be sufficient for this Reynolds number. In the following, only results from this mesh will be shown.

Fig. 3 presents numerical results obtained with RANS and V-LES using different filter widths. If the mean velocities seem to match qualitatively the experiments, with an unsteady flow being established, it can be noticed that in all cases, the recirculation zone is larger than the experiments and previous reported simulations. This means that 2D simulations are probably not sufficient to resolve the flow.

When looking at the results – though quantitatively – it can be seen that the Reynolds stresses are under-estimated in the vicinity of the walls using RANS and V-LES using various filter widths, which, both could be treated in 2D in contrast to LES. In the central part of the flow, the present results match the experiments, except in the wake of the cylinder where a larger recirculation zone is noticed. The results depart from experiments and previous simulations when considering now the turbulent fluctuating quantities. Even if the qualitative behaviour of $\langle u'u' \rangle$ and $\langle v'v' \rangle$ is closer to the experimental results, the magnitude differs by at least 50%. Results of $\langle u'v' \rangle$ are far from the experiment, even qualitatively. It seems that two-dimensional simulations fail to predict the flow near the walls, and that three-dimensional simulations are necessary to capture the full effect of unsteadiness, especially the spanwise unsteadiness. In the above result, we have also noticed that the effect of varying the filter width on the V-LES results could be important. This has led to us to make a systematic sensitivity analysis of this parameter, but in 3D, as discussed next.

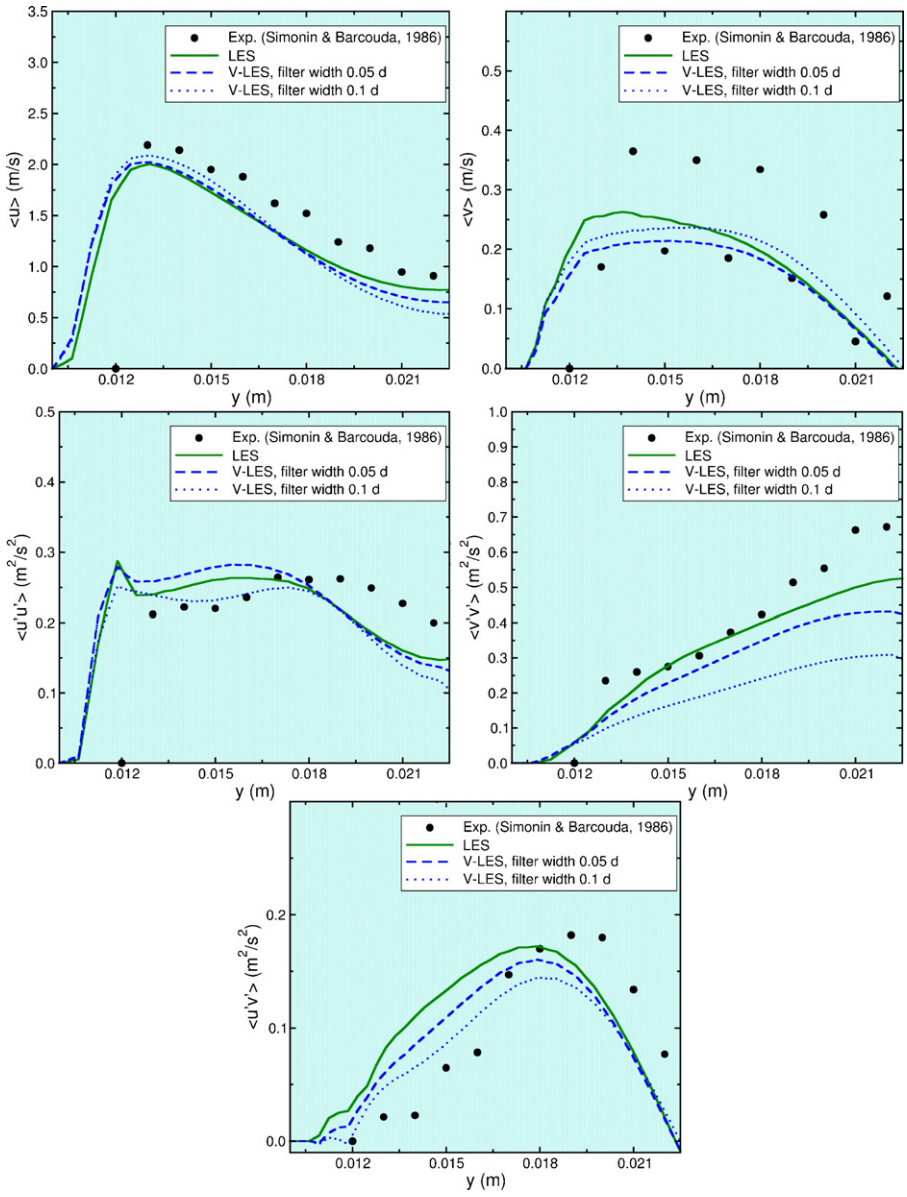

Fig. 7. Comparison of LES and V-LES on a mesh of depth 1.5d, results at $x = 0$ mm.

4.2. 3D simulations

Three-dimensional simulations are reported in this section, for both V-LES and LES, using the same grid. First, the influence of the mesh size is analyzed, for grids of $50 \times 50 \times 20$ and $100 \times 100 \times 43$ cells, with a size of one diameter in the spanwise direction. These meshes are understandably coarse for LES, but cannot be refined further because of the computational costs it implies. In V-LES, the filter width is fixed to 0.1d.

As can be seen in Fig. 4, the size of the mesh has a little influence only on the mean velocities $\langle u \rangle$ and $\langle v \rangle$. In contrast, the results seem to be very different when looking at the Reynolds stresses. It is therefore advised to use a mesh with cell width equal or less than $4.5\,10^{-5}$ m. However, this threshold will not be always respected in the following computations, because of the computational cost involved with such a resolution. Indeed, more than 70 h are needed to simulate the flow during 1 s when using LES for a mesh of $100 \times 100 \times 43$ cells, against less than 12 h when using a mesh of $50 \times 50 \times 20$ cells.

The influence of the filter width for V-LES is now tested, and results are shown in Fig. 5 for a mesh consisting of $100 \times 100 \times 43$ cells. For these simulations the depth of the computational domain in the spanwise direction is one diameter. It can be seen that the filter width of 0.2d provides results that are actually two-dimensional, with large variations in the normal Reynolds stress in the streamwise direction. Results obtained with the filter width of 0.1d do not match the experimental data, particularly when looking at the Reynolds stresses. This behaviour could be explained by the too small depth of our computational domain, which prevents large spanwise structures to develop. A filter width of 0.05d, which would allow the smaller turbulent structures to develop, provides indeed results matching the data and LES.

To confirm this explanation, simulations with different sizes of the computational domain in the spanwise direction have been conducted, with a filter width of 0.1d, and a constant cell size in all directions of 9×10^{-4} mm. Results of this analysis are presented in Fig. 6. It is clear that a depth of only 0.5d prevents three-dimensional structures from developing as was to be expected, and thus, the results are the same as in the two-dimensional simulations. Using

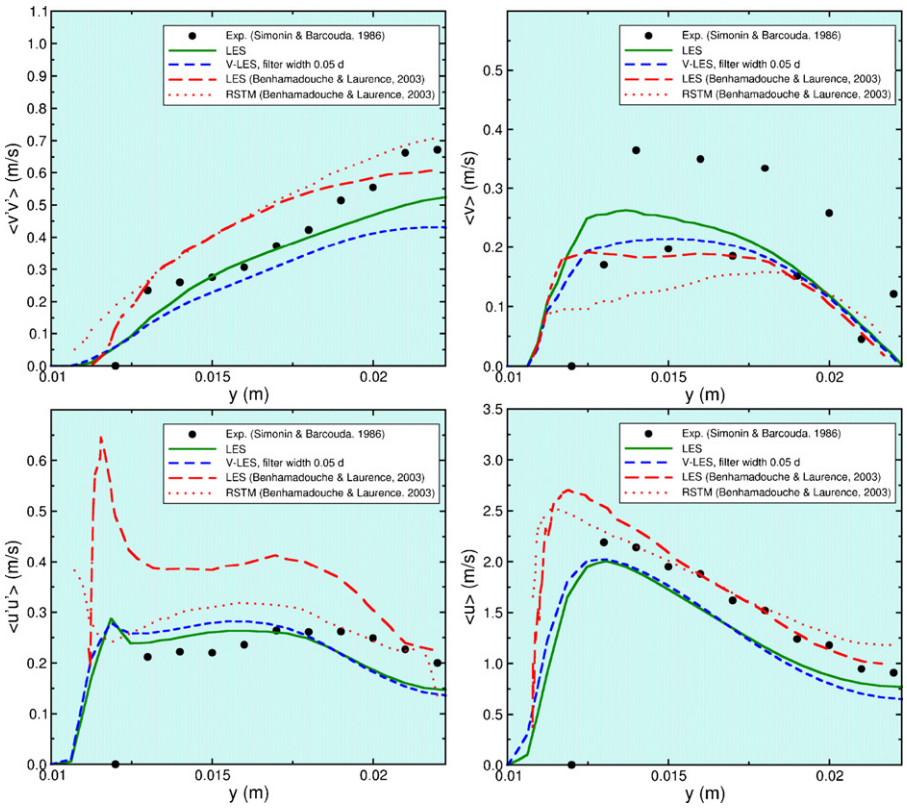

Fig. 8. Comparison between experiments, TransAT LES, V-LES (with filter width = 0.05d) and UMIST LES and RSM. 3D simulations in all cases; results presented at $x = 0$.

a depth of 1d provides better results, but this is still not sufficient, as can be observed when looking at the results for the shear stress. On the other hand, a depth of 1.5d is large enough such that the turbulent structures can develop, and are similar to 2d domain depth. It is therefore recommended to use a depth of the computational domain of at least 1.5d, or larger than 10 times the filter width, at least.

5. Validation against experiments and previous calculations

5.1. Mean velocities and Reynolds stresses

Once the influences of the different computational parameters have been assessed, the V-LES and LES simulations are now compared against the experimental data. Because the previous sensitivity analysis has shown that the depth of the domain may be critical for the solution, and was subsequently increased to 1.5d, the grid resolution in the third direction was therefore increased by factor of 15%. Note that this final mesh resolution has about the same precision as the one used by Benhamadouche and Laurence (2003), albeit with only 20 cells in the spanwise direction.

The results of these final larger-depth simulations are presented in Fig. 7, where two filter-widths have been used, namely 0.05d and 0.1d. Smaller filter-width results 0.05d provide very good agreement with both the present LES results and experiments. Results using a larger filter width of 0.1d deviate slightly from the data, but they still match the measurements when looking at the mean velocities in particular. Both the streamwise normal Reynolds stress and shear stress are remarkably well predicted by V-LES as compared to LES, although the effect of varying the filter width for this depth is noticeable for the cross-flow normal stress mainly.

Comparing now the work with previous other CFD-based findings using high-order turbulence models and LES, the present results are overall very satisfactory. The current results slightly underestimate the streamwise velocity close to the walls as compared to Benhamadouche and Laurence (2003) and Johnson (2008) – though performed in 2D; in both these references, this quantity is rather slightly overestimated, while in contrast Hassan and Barsamian (2004) report very good results in this zone. Our results may be explained by the fact that we do not have cell refinement near the walls. The current prediction for $\langle v \rangle$ is however very good and match that of Benhamadouche and Laurence, and are better that Johnson's (2008) 2D results. The normal stress $\langle u'u' \rangle$ is very well predicted, too, though with departures from measurements with about 10%. The behaviour is better than in Benhamadouche and Laurence (2003) paper, which report a larger peak near the walls. $\langle v'v' \rangle$ is also well reproduced by our V-LES, although being slightly under-estimated in the core-flow region. The same behaviour is reported by Johnson, in contrast to Benhamadouche and Laurence, Hassan and Barsamian who obtained results with close match to the experiment. Finally, though the shear stress shows a good behaviour overall, the quantity is overestimated near the wall and shows a shift of the peak; the same being reported in the LES results of Benhamadouche and Laurence. Hassan and Barsamian report instead a closer match to the experiment.

5.2. Direct comparison with other LES and RSM data

In order to assess the quality of the present LES simulations, our data are compared with those obtained by Benhamadouche and Laurence (2003), using a BFC grid. The comparison is presented in Fig. 8, in which we have added the results of their RSM simulation and our V-LES results. The RSM approach is supposed to yield better results than any RANS model, be it linear or nonlinear. The argument of commercial codes being used does not hold here, since the code used by UMIST is an in-house code,

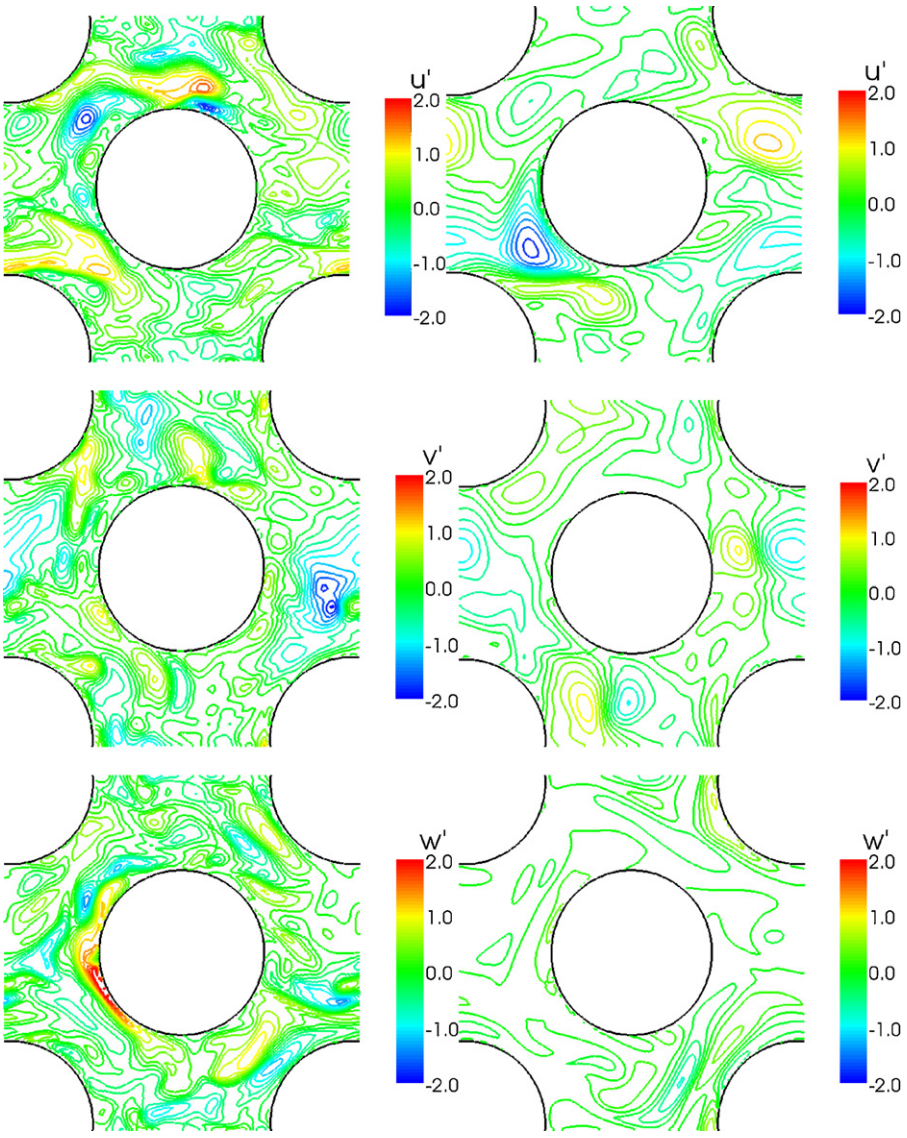

Fig. 9. Flow structures in LES (left) and V-LES (right). Fluctuating velocities u', v' and w'.

validated over hundreds of test cases. The comparison shows first that our LES are way better than their LES, part may be a better behaviour of their model for the $\langle v \rangle$ velocity. Second, it seems that their RSM simulations provide indeed the right trend as compared to experiments, way better than our simple RANS model simulations (see Fig. 3), but the quality is not as good as the present V-LES results. V-LES is clearly superior to any RANS approach, and could even outperform is a more sophisticated sta-

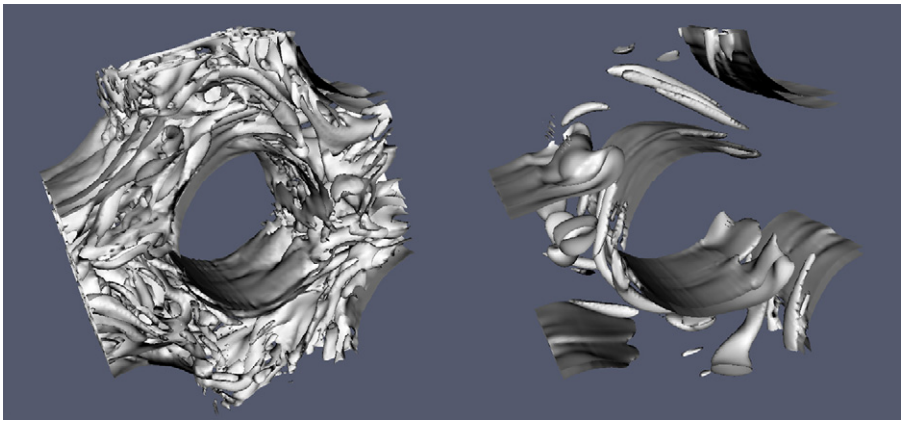

Fig. 10. Instantaneous vorticity field. Comparison between LES (left) and V-LES (right).

tistical model is used in combination with LES, e.g. the RSM or EASM.

5.3. 3D structures of the flow

The turbulent structures of the flow are now are shown in Fig. 9, highlighted by iso-values of the fluctuation velocities u', v' and w'. The figure compares LES and V-LES for a filter width of $0.1d$. It can be seen that the V-LES (right panels) reproduces indeed the three-dimensional structures, but they are not as fine as in the LES (left panels). The difference in the size and shape of the structures is further illustrated by reporting iso-values of the total vorticity in Fig. 10. This difference in the size of the turbulent structures explains the different conclusions drawn between the present work and that of Rollet-Miet et al. (1999) – also based on 3D LES – on the size of the domain in the spanwise direction: they found indeed that a depth of one diameter was sufficient for their LES simulations, whereas a depth of at least 1.5 diameter is shown to be needed for both the V-LES and LES to capture the three-dimensional structures. The present result suggests that the large scales are the most important contribution to turbulent kinetic energy, which makes of the V-LES a very good alternative to LES, at least for this class of flow. The benefit of the V-LES is mainly in reducing the CPU time needed for full 3D LES. The fining points out to the fact that SGS models of various sophistication will not necessarily bring a marked difference compared with a simple models.

6. Conclusions

In this study V-LES and LES approaches have been applied for a flow across a tube bundle. The first conclusion to be drawn is that the flow must be resolved in three-dimensions, under transient conditions, with refined grids, in line with previous CFD studies on this subject. Indeed, three-dimensional structures, which play a major role when evaluating the Reynolds stresses, cannot arise in two-dimensional simulations. Very Large Eddy Simulation has been tested, validated, and thoroughly assessed by varying various computational parameters: grid, filter width, domain size, and inflow conditions. This model or rather modelling approach is proved to provide the flow unsteadiness in three-dimensions, while saving computational cost compared to Large Eddy Simulation. The simulation results obtained with V-LES are very satisfactory when compared with the data and available calculation results from various other sources. As expected, the method is computationally efficient (it can be applied using an implicit solver which permits a higher CFL than with LES; typically CFL$\sim$1 against $\sim$0.1), and numerically robust. The computational cost decreases with increasing filter width, though at the expenses of the quality of the results. The RSM simulations of this flow provide the right trend as compared to experiments, way better than simple RANS model simulations, but the quality is not as good as the present V-LES results. V-LES is clearly superior to any RANS approach, and could even outperform if a more sophisticated statistical model is used in combination with LES, e.g. the RSM or EASM. Another advantage of the model as shown here is that it could be degenerated to a DES to better treat high-lift aerodynamics flows.

In the light of this systematic assessment investigation, V-LES seems to be a good compromise between efficiency and precision, and thus may be used for industrial applications under high-to-very-high Reynolds number, where LES will always remain expensive (to obtain statistically convergent results). Not limited to turbulent single phase flows only, V-LES has been recently shown to be extendible to multiphase flow systems, including steam–water systems such as pressurized thermal shocks and gas–liquid stratified flows in pipes and ducts (Lakehal and Labois, 2011).

Acknowledgements

The work was conducted using the TransAT code of ASCOMP within NURISP; an EC-funded project in the framework of the 7th EURATOM Framework Program. The authors are grateful to Prof. D. Laurence (UMIST) for having shared his data with us.

References

ASCOMP GmbH, 2009. Multi-Fluid Navier-Stokes Solver TransAT User Manual.
Benhamadouche, S., Laurence, D., 2003. LES Coarse LES, and Transient RANS comparison on the flow across a tube bundle. International Journal of Heat and Fluid Flow 24, 470–479.
Hassan, Y.A., Barsamian, H.R., 2004. Tube bundle flows with the large eddy simulation technique in curvilinear coordinates. International Journal of Heat and Mass Transfer 47, 3057–3071.
Johansen, S.T., Wu, J., Shyy, W., 2004. Filtered-based unsteady RANS computations. International Journal of Heat and Fluid Flow 25, 10–21.
Johnson, R.W., 2008. Modeling strategies for unsteady turbulent flows in the lower plenum of the VHTR. Nuclear Engineering and Design 238, 482–491.
Lakehal, D., Thiele, F., 2001. Sensitivity of turbulent shedding flows to non-linear stress–strain relations and Reynolds stress models. Computers and Fluids 30, 1–35.
Lakehal, D., Labois, M. A New modeling strategy for phase-change heat transfer in turbulent interfacial two-phase flow. IJMF, (available online) 2011, doi:10.1016/j.ijmultiphaseflow.2011.03.004.
Launder, B.E., Spalding, D.B., 1974. The numerical computation of turbulent flows. Computer Methods in Applied Mechanics and Engineering 3, 269–289.
Moulinec, C., Pourquié, M.J.B., Boersma, B.J., Buchal, T., Nieuwstadt, F.T.M., 2004. Direct numerical simulation on a Cartesian mesh of the flow through a tube bundle. International Journal of Computational Fluid Dynamics 18 (1), 1–14.
Nicoud, F., Ducros, F., 1999. Subgrid-scale stress modelling based on the square of the velocity gradient tensor. Flow, Turbulence and Combustion 62, 183–200.
Norris, L.H., Reynolds, W.C., 1975. Turbulent Channel Flow with a Moving Wavy Boundary, Rept. No. FM-10, Stanford University, Dept. Mech. Eng.
Peskin, C.S., 1972. Flow patterns around heart valves – numerical method. Journal of Computational Physics 10 (2), 252–271.
Rollet-Miet, P., Laurence, D., Ferziger, J., 1999. LES and RANS of turbulent flow in tube bundles. International Journal of Heat and Fluid Flow 20, 241–254.
Ruprecht, A., Helnrich, T., Buntic, I., 2003. Very Large Eddy Simulation for the prediction of unsteady cortex motion. In: Symposium of the 12th International Conference on Fluid Flow Technology , Budapest, Hungary.
Simonin, O., Barcouda, M., 1986. Measurements of fully developed turbulent flow across tube bundle. In: Third International Symposium on Applications of Laser Anemometry to Fluid Mechanics , Lisbon, Portugal, pp. 21.5.1–21.5.5.
Smith, L.M., Woodruff, S.L., 1998. Renormalization-group analyzes of turbulence. Annual Review of Fluid Mechanics 30, 275–310.
Spalart, P.R., Allmaras, S.R., 1992. A One-Equation Turbulence Model for Aerodynamic Flows, AIAA Paper 92-0439.
Speziale, C.G., 1998. Turbulence modelling for time-dependent RANS and VLES: a review. AIAA Journal 36 (2), 173–184.